Nanomed Res J 6(2):128-147, Spring 2021

RESEARCH ARTICLE

Green synthesis and characterization of zinc oxide nanoparticles using *Berberis tinctoria* Lesch. leaves and fruits extract of multi-biological applications.

Arumugam Vignesh[1], Subramaniam Selvakumar[2], Krishnan Vasanth[1*]

[1] Department of Botany, Bharathiar University, Coimbatore 641 046, Tamil Nadu, India.

[2] Department of Biochemistry, Bharathiar University, Coimbatore 641 046, Tamil Nadu, India

ARTICLE INFO

Article History:
Received 19 Jan 2021
Accepted 26 Mar 2021
Published 01 May 2021

Keywords:
Berberis tinctoria
ZnO NPs
Antibacterial
Anti-biofilm
Antioxidants
Anti-cancer

ABSTRACT

The green synthesis of zinc oxide nanoparticles (ZnO NPs) was rendered by using *B. tinctoria* leaves and fruit extract. These extracts acted as a capping and reducing agent in stabilizing the development of ZnO NPs. The obtained NPs were characterized by using absorption spectroscopy analysis (UV-vis) and Fourier-transform infrared spectroscopy (FT-IR) which showed a distinct peak at 274 nm, 467cm-1, and 456 cm-1 Further, the formation has been confirmed by powder X-ray diffraction (XRD) and the obtained XRD pattern fitted well with the JCPDS card, showing the pure crystalline nature of synthesized NPs Patten. The Scanning Electron Microscopy (SEM) analysis revealed hexagonal particle shape and Energy Dispersive X-ray (EDX) by confirming the strong signals of Zinc and oxygen. The results of Dynamic Light Scattering (DLS) showed that NPs obtained from both NPs of 244nm and 256nm size with the surface zeta potentials of -15.0mV and -18.9mV. Antibacterial and anti-biofilm efficacy of synthesized nanoparticles were evaluated against six human pathogenic bacteria, resulted that antibacterial/anti-biofilm activity was increased upon increasing the concentration dose range. The obtained NPs exhibited significant antioxidants potential, which was made to study the anticancer activity against Raw 264.7 and Caco-2 cancer cell lines, which showed absolvable activity.

How to cite this article
Vignesh A., Selvakumar S., Vasanth K. Green synthesis and characterization of zinc oxide nanoparticles using Berberis tinctoria Lesch. leaves and fruits extract of multi-biological applications. . Nanomed Res J, 2021; 6(2): 128-147. DOI: 10.22034/nmrj.2021.02.005

INTRODUCTION

Nowadays, the demand for the modern lifestyle is rising day by day therefore, numerous technologies were needed to rectify health care issues to provide a sustainable environment for all living things [1]. Nanoscience is an advanced applied science for expanding research area by synthesized new novel materials in small sizes with different shapes with high surface area [2]. The magnetic nanoparticles are synthesized conventionally due to their broad range of distribution in an array of applications by various methods as microwave-assisted synthesis, chemical methods, and hard template directing techniques, sol-gel, and thermal methods. The chemical synthesis method leads to the production of toxic chemical byproducts or high temperature and pressure [3, 4]. However, regular experimental techniques have the potential risk to cause hazardous effects to the environment involving the utilization of organic solvents, high reactive reducing, and capping agents [5]. Therefore, the green synthesis of nanoparticles has been proposed as an eco-friendly alternative to chemical and physical methods using microorganisms, alga, enzymes, and plants [6], especially the plant-based biosynthesis has fewer cross contaminations. The ZnO NPs are focused by the researchers to utilize in industries and clinical areas. Which possesses high electron mobility, high transmittance, and versatile semi-conductance at room temperature with increased excitation binding energy [7]. In many fields such as biomedical, bio-sensing, drug delivery, food packing, cancer therapy, agriculture,

* Corresponding Author Email: *vasanthlabbu@gmail.com*

cosmetics, and various other fields [8]. The pharmaceutical sciences are using nanoparticles to reduce the toxicity levels and after-effects of the drug. Therefore, new strategies are needed to identify and develop the next generation of drugs.

Infectious diseases account for a high proportion of health problems and a huge amount of antibiotics are consuming to fight infections, moreover, bacteria have the potential to develop resistance against antibiotics [9]. Antimicrobial resistance has turned into a global health issue, which MDR (Multiple Drug Resistance) bacteria are posing a problem in the treatment and control of infectious diseases. During this millennium, overcoming resistance to antibiotics is one of the major issues faced by a human. Quorum sensing is a cell to cell communication for the different virulent gene expressions such as proteases, pyocyanin, toxic, and biofilm formations. It has no interference with growth but there is a probability of developing resistance against them [10]. However, pathogenic microorganisms can protect themselves against inhibitory compounds by the development of biofilms [11]. Biofilms are assemblages of microbial cells embedded in a matrix of self-produced polymeric substances such as polysaccharides, proteins, and DNA. They are found adhering to both biological along with non-biological surfaces [12]. It has been stated that microbial biofilms are involved in chronic infectious diseases in humans, estimated at around 65 % of all infections in line with the Centre for Disease Control (CDC) [13]. Biofilms can also be seen in Planktonic cells, medical implants, living tissues and urinary catheters form biofilms, they can become more resistant to antibiotics [14]. It has been confronting that ZnO NPs exhibits antimicrobial activity by rupturing the integrity of bacterial cell membranes, decreasing cell-surface hydrophobicity, and downregulating the transcription of oxidative stress, which also act as a resistance to genes in bacteria [15]. It inhibits the actuation and proliferation step of the reaction and delays the oxidation process leads to end of the reaction.

Indian traditional healthcare system used diverse medicinal plants for thousands of years cause of its phytocompounds with interesting antioxidant activities. The previous reports of biosynthesized NPs using plant-based showed more antioxidant activity compared to chemical synthesis methods [16]. The antioxidants are known to have protective activity against the free radicals damage and reactive oxygen species. In the 21st century, nanotechnology is anticipated to be the basis of many biotechnological innovations also the nanomaterial is developing the base in modern medicine techniques [17, 18]. Proves to be highly efficient, stable, low-cost, soluble, and non-toxic, and simultaneously it is easy to outreach the targeted area. Nanomedicine was found to treat cancer at its early stage [19].

Berberis tinctoria is an evergreen shrub; endemic to Southern Western Ghats, predominantly found at the higher altitude of the Nilgiris, Tamil Nadu, India. It belongs to the family Berberidaceae, grows 2 to 3 feet in height and it reaches15 feet in the forest, with a hard stem having long limited branches with numerous slender leafy twigs [20]. The leaves and fruits are chiefly consumed raw by the tribal and rural people of the Nilgiris for many diseases, which are not scientifically reported. *Berberis* genus has numerous well-known medicinal plants used on the account of ancient times as a remedy for gall balder stones, eye disease, jaundice, rheumatism, diabetes, fever, kidney stone, vomiting during pregnancy, and varied ailments [21]. The present work reports the synthesis of ZnO NPs from a principal medicinal plant, *B. tinctoria*. Characterization of ZnO NPs was done by using UV–visible spectroscopy, XRD, SEM, EDX, DLS, and ZETA potential measurement. The ZnO NPs had antioxidant activity, antibacterial, and anti-biofilm activity against the human pathogenic bacterium. Furthermore, we investigated the cytotoxicity activities of the ZnO NPs against RAW 264.7 (Mouse leukemic monocyte-macrophage cells) and Caco2 (human colonic adenocarcinoma cells) cell lines. To the preeminent, the *B. tinctoria* has been used earliest to synthesis ZnO NPs, an attempt was made to green synthesis characterization and assessment of their effects on biological activities

MATERIALS METHODS

Collection and identification of plant material

The plant *B. tinctoria* was collected from Doddabetta, 11°24'08.7"N 76°44'12.2"E (2623 meters i.e., 8652 feet above mean sea level the Nilgiris, Tamil Nadu, India. The fresh leaves and fruits were collected from December 2018 to May 2019. The taxonomic identity of the plant was confirmed and certified by the Botanical Survey of India, Southern Regional Centre, Coimbatore, Tamil Nadu, India (BSIS/RC/5/23/2016/Tech./164).

Preparation of leaf and fruit extracts

The leaves and fruits were collected and washed thoroughly under running tap water. It was then washed using deionized water and air dry at room temperature. Afterwards, 20 g of both leaves and fruits were finely cut into small pieces and soaked in 100 mL of double-distilled water. The samples were heated at 60°C for 10 min until the brown color was obtained and cooled at room temperature. Further, it was filtered using Whatman number-1 (40) filter paper and then stored at 4°C for further use.

Synthesis of zinc oxide nanoparticles

The ZnO NPs were synthesized stated to the modified protocol developed by [22]. Initially, 30 mL of leaf and fruit extracts were heated to 70°C under constant stirring by adding 0.1 M Zinc acetate dihydrate and 1 M Sodium hydroxide (NaOH) solution to appear a deep yellow-colored precipitate. Afterwards, the precipitate was pelleted down by centrifuging at 6000 rpm for 20- 25 min. The pellet was washed several times thoroughly using Milli- Q Water and ethanol. Finally, the pellet was dried at 40°C for 8 hours in a hot air oven to get maximum yield. The powder material was smashed using mortar and pestle to obtain a uniform size. Further, NPs were used for characterization and biological activities.

Characterization

The UV-vis absorption spectra of synthesized ZnO NPs samples were recorded by using an 1800 Shimadzu UV- vis Double beam spectrophotometer with a wavelength range was 200 to 700nm. The XRD patterns of the biosynthesized ZnO NPs powder have been analyzed with the help of the PAN analytical Xpert Pro Model (Netherlands) which was operating at 45 kV, 40 mA, with Cu Kα radiation at θ -2θ angles (0-80° range). Scherrer's equation was used to calculate the average crystallite size of ZnO NPs.

Formula: $d\ 0.9\lambda/\beta_{1/2}\cos\theta =$

Where, d = crystallite size, λ = X-ray wavelength (CuK α),

β1/2 = Full width half maximum (FWHM) and θ = diffraction angle.

The chemical bonds of biosynthesized ZnO NPs were recorded by (FTIR, Bruker Tensor 27 spectrometer, Bremen, Germany) Fourier transform infrared techniques in the range of 400 cm-1 -4000 cm-1. The morphology of biosynthesized ZnO NPs was captured using FEI QUANTA 200 at 400 µm and 5 µm. The thin films of the sample were prepared on a copper grid coated with carbon by dropping 20-50 µl of sample on the grid and observed under the analyzer. The excess material was cleaned with tissue and then dry under a mercury lamp for 4- 5 min. Electron Diffraction Spectroscopy (EDX) patterns were recorded by the JEOL/EO JSM-5600 SEM microscope along with an energy dispersive X-ray spectrometer. Dynamic light scattering (DLS) and zeta potential of biosynthesized ZnO NPs were analyzed to know the average size and stability of particles, Zetasizer Nano ZS90 (Malvern Instruments Ltd., Malvern, UK) DLS assumes on the interaction of nanoparticles with lights and a DLS measurement mostly relies on Rayleigh scattering from the particle size and zeta potential in liquid suspension were both measured at 25°C. The sample size for surface zeta potential measurement was limited to no larger than 4 mm × 7 mm × 1.5 mm (L × W × H).

Anti-bacterial studies

Microbial culture, growth medium, and culture conditions

Staphylococcus aureus (MCC 2408), *Escherichia coli* (MCC 3105), *Salmonella typhi* (MTCC 3224), *Pseudomonas aeruginosa* (MCC 3462), *Enterococcus faecium* (MCC 3545), and *Enterococcus faecalis* (MCC 3049) strains were grown in Mueller- Hinton medium (MHA) at 35±2°C and 180 rpm. MHA medium composition (Beef extract- 2.00 gm, Acid hydrolysate of casein- 17.50 gm, Starch- 1.50 gm, and Agar- 17.00 gm) were dissolved in 1L sterilized distilled water and then adjusted to pH 7.3 ± 0.1 before sterilization.

Anti-bacterial activity of biosynthesized ZnO NPs of an agar well diffusion method:

Antimicrobial activity of the biosynthesized ZnO NPs was performed against six human pathogenic bacteria (three gram-positive and three gram-negative). Anti-bacterial agar well diffusion method followed by [23] with some modifications. The pure cultures of organisms were subcultured in Mueller- Hinton broth at 35 ± 2°C for 24h. 100µL of a fresh culture of each test organism was dispersed over the nutrient agar plates with a sterile glass rod. The plates were dry for 10 min and make5 mm wells into the agar plates. The wells were secured with a drop of molten agar (0.8 %) to prevent nanomaterials discharge from the bottom of the well. Then, the

different concentrations ZnO NPs were prepared (50,100, and 150 µg/mL) of the sample preparation, 10 µL of tetracycline (positive control), and 50 µL of sterile distilled water (negative control) was poured into each well on the plats. After (35 ± 2°C) overnight incubation, the different levels of the zone of inhibition were measured.

Anti-biofilm activity

The biosynthesized ZnO NPs were used as anti-biofilm agents against six human pathogenic bacteria (100 µL of bacterial culture was added into sterile test tubes containing 5 mL of sterile Mueller-Hinton broth). Subsequently, sub-MIC doses (0, 10, 20, 30 µg/mL) of ZnO NPs were added to each test tube excluding the control set where only the bacteria was grown in absence of ZnO NPs. All the test tubes were then incubated at 35±2°C for 48 h. After the incubation time, the planktonic cells were discarded from each test tube and residual cells were washed twice with distilled water. Thereafter, each tube was stained for 15 min with 0.4 % of crystal violet solution at room temperature for biofilm identification. After that, the tubes were washed with distilled water. Then, 5 mL of 33 % glacial acetic acid was added to dissolve the adsorbed crystal violet (CV) and the intensity was quantified by measuring the absorbance at 420 nm. To confirm the CV assay biofilm morphology was examined by microscopy. Sterile coverslips were added in each tube and the above incubation methodology was followed. After the desired incubation period coverslips were aseptically taken out from each test tube and stained with (0.1 %) crystal violet and 0.4 % acridine orange separately to examine the extent of biofilm association of light microscopy [24].

Antioxidant activities

DPPH scavenging activity

The hydrogen donating or radical scavenging ability (antioxidant activity) of the sample was estimated in terms of using the stable radical 2, 2-diphenyl-1-picrylhydrazyl (DPPH). The leaves and fruits-based biosynthesized ZnO NPs were taken in aliquot concentrations and the final volume was made to 100 µL with methanol. About 3 mL of a 0.1 mM DPPH methanolic solution was added to the tubes and vortexed well. Then 3 mL DPPH methanolic solution with 100 µL methanol was prepared as a negative control and standard butylated hydroxytoluene (BHT) and Ascorbic acid (Concentration 0- 15 µM). After dark incubation of 30 min at room temperature, the absorbance of the sample was measured at 517 nm against the blank. The DPPH radical quenching results were expressed as IC_{50} values [25].

ABTS scavenging activity

ABTS (2, 2' azino-bis 3- ethylbenzothiazoline-6-sulphonic acid) radical assay by cation decolorization [26] was used to measure the total antioxidant activity of biosynthesized ZnO NPs. 7 mM ABTS with 2.4 mM potassium persulfate reacting in the dark for 12- 16 hours at room temperature and diluted in ethanol (about 1: 89 v/v) to give an absorbance of 0.700 ± 0.02 at 734 nm at 25**°C**. 1 mL of diluted ABTS solution was added to standards (BHT and Rutin (Concentration 0- 15 µM) and samples, then incubated at 30**°C** exactly for 30 min and the absorbance was measured at 734 nm. The results were expressed in µM Trolox equivalent antioxidant capacity (TEAC) per sample extracts (µM/g).

Phosphomolybdenum assay

The total antioxidant activity of biosynthesized ZnO NPs was evaluated by the phosphomolybdenum method [27]. The biosynthesized NPs solutions and ascorbic acid (10- 50 µg) were incorporate with 1 mL of reagent (0.6 M sulphuric acid, 28 mM sodium phosphate, and 4 mM ammonium molybdate). The tubes were incubated at 95**°C** for 90 min in a water bath and rest to room temperature. The standards BHT and Ascorbic acid were used (Concentration 0- 15 µM). The absorbance was measured at 765 nm against a reagent blank and expressed in mg ascorbic acid equivalents per gram sample extract (mg/g).

Ferric reducing antioxidant power (FRAP) assay

The ability to reduce TPTZ- Fe (III) complex to TPTZ- Fe (II) complex by the antioxidant capacity of green synthesized ZnO NPs are estimated according to the procedure [28]. Freshly prepared FRAP reagent (900 µL) (2.5 mL of 20 mM/L TPTZ (2, 4, 6-tripyridyl-s-triazine) in 40 mM/L HCl and 2.5 mL of 20 mM/L $FeCl_3$-$6H_2O$ and 25 mL of 0.3 M/L acetate buffer (pH 3.6)) incubated at 37**°C**. Then the FRAP reagent was added to biosynthesized ZnO NPs, the aliquots of butylatedhydroxytoluene (BHT) and Ascorbic acid (10- 50 µg); then to the methanol served as the reagent blank. All these tubes were incubated at 37**°C** for 30 min in a water bath. The absorbance of the blue color was

read against the reagent blank at 593 nm and the results were reported mM Fe (II)/ mg extracts.

Metal chelating activity

Biosynthesized ZnO NPs has ferrous ions, the chelating activity of these ions was determined by [29]. About 2 mM 100 µL ferrous chloride was added to 500 µg of sample extracts and 400 µL of 5mM ferrozine later to initiate the reaction, then incubated at room temperature for 10 minutes. The absorbance was measured spectrophotometrically at 562 nm against deionized water as a blank and EDTA (10- 50 µg) was used as the standard metal chelating agent. The results were expressed as mg EDTA equivalents per gram sample extracts.

Cell culture maintenance

The cytotoxicity activity of green synthesized ZnO NPs by using the MTT assay method to investigate the toxicity level. A commercially purchased Raw 264.7 (mouse leukemic monocyte-macrophage cells) and Caco-2 (human colonic adenocarcinoma cells) from National Centre for Cell Sciences (NCCS), Pune, Maharashtra, India. The cell culture 1 X 105 cells were seeded in 96 well plates and allowed to settle down for 12 hours. The cultured in Dulbecco's Eagle's medium (DMEM), supplemented with 10% v/v Fetal Bovine Serum (FBS), 2mM l-glutamine, 40 µg/mL gentamycin, 100 U/mL penicillin and 1040 µg/mL Streptomycin. The culture was maintained at 37°C with 5 % CO_2, 85 % humidity. The medium was changed the alternative day, and confluent cells were used for further experimental analysis.

In vitro cytotoxicity by MTT assay

The (3-(4,5-Dimethyl-2-Thiazolyl)-2,5-Diphenyl-2H-Tetrazolium Bromide (MTT) assay developed by [30]. The cells were seeded in a 96 well plate and allowed to settle down for 12 hours. The test solution (leaves and fruits) ZnO NPs were prepared in different concentrations ie,.0, 25, 50, 75, 100, 125, 150, 175, 200 µg/mL with 100 µl DMEM, 0.01% DMSO devoid of FBS. The cells were exposed for 24 hours and control was devoid of NPs. The supernatant was then replaced with 100 µL of MTT solution (5 mg/ mL in PBS) and incubated for 3 h at 37 °C. Subsequently, the formazan crystals (reduction product of MTT) were dissolved in 100 µL of DMSO, and absorbance was measured by the multi-plat reader at 570 nm. The images were viewed using an Olympus CKX41 microscope and were photographed under 400× magnification.

Statistical analyses

All the *in vitro* assays were conducted in triplicates and the results were expressed as Mean ± Standard deviation (SD). The statistical analysis was done using one-way ANOVA and significant differences were determined by the DMRT post hoc multiple comparison test and a value of $p < 0.05$ was considered significant. All calculations were performed using: SPSS, version 20.0 (IBM SPSS, IBM Corp., Armonk, New York).

RESULTS AND DISCUSSION

For the first time, ZnO NPs synthesis was carried out using *B. tinctoria* leaf and fruit extracts via an environmentally benign synthesis method. The formation of ZnO NPs was visually evident from the color change of the reaction mixture from light yellow to dark brown color after 3 hours of reaction and a white powder of ZnO NPs was collected after drying at 60°C in a hot air oven. The synthesized ZnO NPs were used to study its potential against various biological activities.

UV- visible spectral analysis

The UV-vis absorption spectra of synthesized ZnO NPs using leaf and fruit extracts of *B. tinctoria* are shown in **(Fig- 1 a- b)**. ZnO NPs have free electrons, which brings to a surface Plasmon resonance (SPR) absorption band, owing to the combined absorbance of photons of metal nanoparticles in resonance with the light wave. The green synthesis of ZnO NPs was observed at 274 nm in both extracts. The peak of surface plasmon resonance clarified the formation of NPs. The high intensity of UV-vis spectra clearly showed a high intensity of ZnO NPs present in the samples. The obtained results were reconciled with the results already reported for *Scadoxus multiflorus* leaf powder aqueous extracts [31].

FT- IR

In order, to know the functional groups present in the leaves and fruits extracts of *B. tinctoria* ZnO NPs were recorded in **Table- 1** and **Fig-1 c, d.** The IR spectrum showed a broad peak corresponded to O-H stretching frequency of 3455 cm^{-1} and 3410 cm^{-1} confirmed the presence of OH group with either intramolecular or intermolecular hydrogen bonding. A frequency at 1604 cm^{-1} and 1610 cm^{-1} responding C=C stretching in conjugated alkene

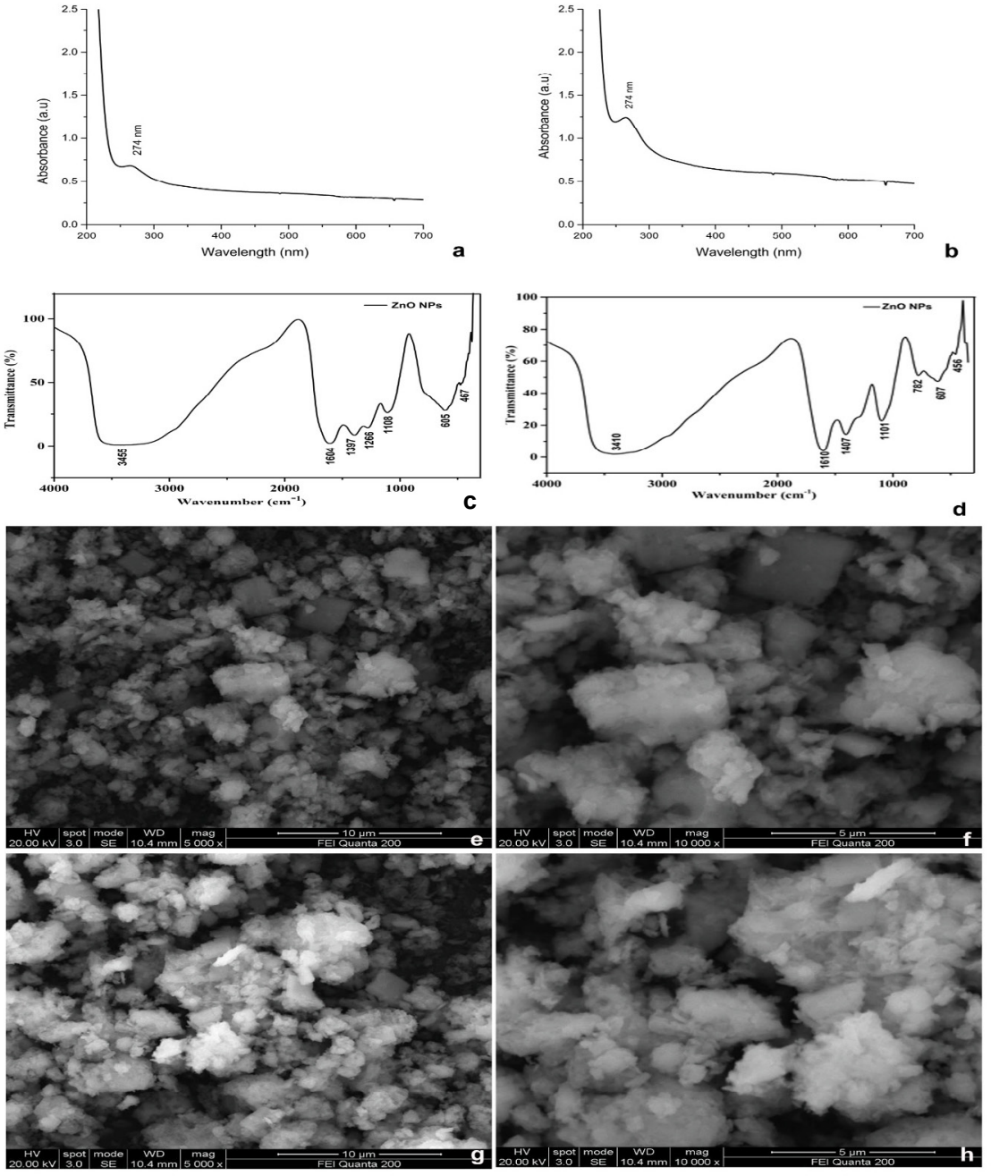

Fig. 1. **a** and **b** UV- Vis spectra of green synthesized ZnO NPs leaf and fruit based synthesis. **c** and **d** FTIR spectrum of green synthesized ZnO NPs leaf and fruit based synthesis. **e- h** SEM image of green synthesized ZnO NPs leaf and fruit based synthesis in different magnification ranges **e** and **g**- 100µm and **f** and **h**- 10µm.

and α, a β-unsaturated ketone of leaf and fruit extract respectively. Further, this has been established with the O-H bending vibrations obtained at 1397 cm^{-1} and 1407 cm^{-1} of leaves and fruits extract by its medium intensity band. The spectrum was also observed in the presence of C-N stretching by week band at 1266 cm^{-1}. The stretching vibrations at 1101 cm^{-1} and 1108 cm^{-1} were carefully assigned the presence of C-O stretching. A peak obtained at 782 cm^{-1} may be aggregated to C-H bending vibrations of fruit extract respectively. there is a noticeable study band was observed at 617 cm^{-1} and 611 cm^{-1}

Table 1. FTIR spectra with possible assignments using Leaf and fruit based biosynthesis ZnO NPs .

Berberis tinctoria Extracts		Frequency (cm^{-1})	Intensity	Possible assignments
Leaf	1	3455	strong	O-H stretching alcohol
	2	1604	medium	C=C stretching in conjugated alkene
	3	1397	medium	O-H bending carboxylic acid
	4	1266	strong	C-N stretching in aromatic amine
	5	1108	strong	C-O stretching tertiary alcohol
	6	605	strong	C-Br stretching in halo compounds
	7	467	strong	Zn-O bond
Fruit	1	3410	strong	O-H stretching alcohol
	2	1610	strong	C=C stretching α,β-unsaturated ketone
	3	1407	medium	O-H bending carboxylic acid
	4	1101	strong	C-O stretching tertiary alcohol
	5	782	strong	C-H bending of 1,2,3, trisubstituted
	6	607	strong	C-Br stretching in halo compounds
	7	456	strong	Zn-O bond

of leaves and fruits extract respectively assigned to the presence of either C-Br or C- Cl band, A Zn-O stretching frequency was found at 467 cm^{-1} and 456 cm^{-1} established the formation of ZnO NPs. This is consistent with the reported ZnO NPs which were prepared from *Berberis aristata* [32].

SEM and EDX

The surface morphology and size of the ZnO NPs. were confirmed by SEM which revealed the hexagonal particle backing. The SEM images at high magnifications at10 μm and 5 μm showed the aggregates of nanocrystallites (**Fig-1 e- h).** The average diameter of the nanoparticle was in the range of 30-50 nm, The EDX spectrum revealed a strong signal for the Zinc **Fig-2 a- b.** The EDX was executed to confirm the elemental composition from leaves and fruits ZnO NPs, which showed Zinc (16.59 %), Oxygen (83.41 %), and Zinc (42.64 %), Oxygen (57.36 %) respectively, the results confirmed the formation of ZnO NPs.

XRD analysis

X-ray diffraction is a versatile, non-destructive analytical method for the identification and quantitative determination of various crystalline forms, known as phases of compound present in the biosynthesized of ZnO NPs using leaves and fruits extract of *B. tinctoria* (**Fig- 2. c, d).** The detected peaks corresponding to the hexagonal phase in leaves based ZnO NPs are found in the lattice planes (h,k,l) 100, 002, 101, 102, 110, 103, and 112 in the 2θ value (27.60°, 29.37°, 32.24°, 44.71°, 53.18°, 59.76° and 64.39° respectively. Even though fruit-based are found in the lattice planes (h,k,l) 100, 002, 101, 102, 110, 103, and 112 in the 2θ value (26.38°, 29.27°, 32.99°, 44.32°, 52.36°, 59.21° and 64.02°. All these peaks are well corresponding to the standard JCPDS file no.36-1451. The peaks confirmed the formation of ZnO NPs with different sizes and similar XRD patterns were also reported in the litterateurs. The more mentioned peak at 32.24° indexed (101) of the wurtzite crystal structure of ZnO. The broadening of peaks in the XRD patterns of ZnO NPs is attributed to variations in the particle size shown in **Table-2.** Scherrer's equation was used for the average size of leaves (5.20 nm) and fruits (3.89 nm) ZnO NPs crystallite size.

DLS and Zeta potential determination

The biosynthesized ZnO NPs using the extracts of *B. tinctoria* (leaves and fruits) NPs size and stability were determined by DLS **(Fig-2 e, f**) and ZETA potential measurement **(Fig-2 g, h**). Since it specifically measures the fluctuations of intensity of the scattered light due to diffusing particles, the determination of the diffusion coefficient of the particles was used for the stability of the particles. It resulted whether the particles aggregate over time by measuring the hydrodynamic radius of the particle increases, particle aggregation shows a larger population with a larger radius. The measurement was done in the liquid condition of ZnO NPs with a pH of 6.4. Zeta potential is the interfacial double layer (DL) electric potential at the slipping plane versus a point in the bulk fluid away from the interface [33]. The magnitude of the zeta potential (-30 mV to +30 mV) gives information about the potential stabili-

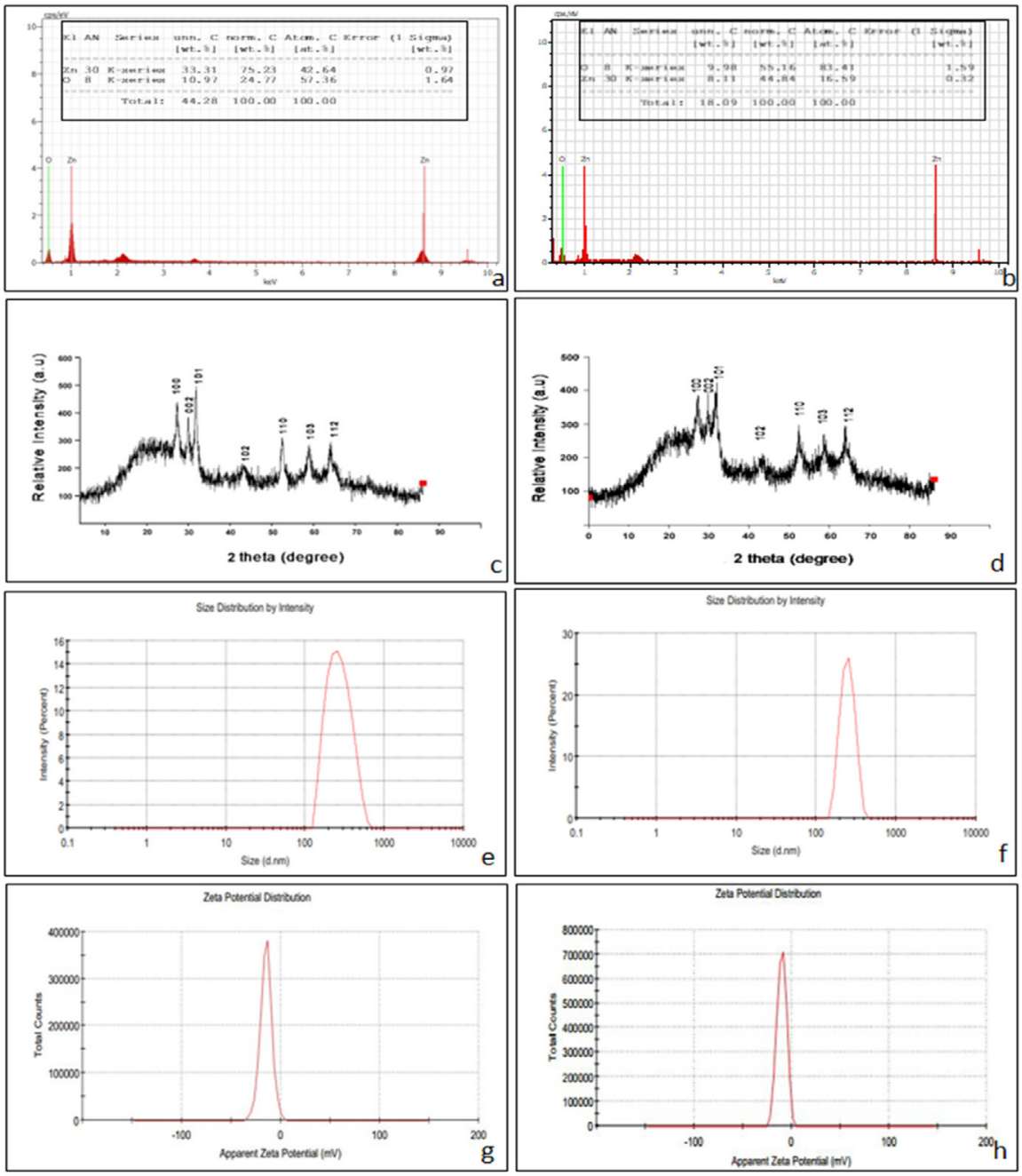

Fig. 2. **a and b** Energy dispersive X-ray spectroscopy (EDX) of green synthesized ZnO NPs leaf and fruit based synthesis. **c** and **d** X ray diffraction (XRD) analysis of green synthesized ZnO NPs leaf and fruit based synthesis. **e** and **f** size distribution and **g** and **h** zeta potential of ZnO NPs determined by dynamic light scattering of leaf and fruit based synthesis.

ty of the colloidal solution [34]**.** The high negative and larger hydrodynamic value of zeta potential confirmed that the repulsion among the NPs and thereby increase the stability of the formulation, wherever the agglomerates of ZnO NPs rather than aggregates in the aqueous condition. The observed negative potential indicates maybe due to the presence of various natural product constituents which were acting as reducing agents in the extracts [35]. Also, it confirmed the presence of gross electrostatic forces within the synthesized material. The zeta potential value of leaves and fruits was found to

Table 2. Crystalline size of ZnO nanoparticles synthesized using *Berberis tinctoria* leaf and fruit extract.

Berberis tinctoria Extracts		2θ value (degree)	d-Spacing (A	Plane (hkl)	FWHM (degree)	Cos θ	Crystalline size only (nm)
Leaf	1	27.60°	2.9921	(100)	1.6875	13.63	4.86
	2	29.37°	2.5800	(002)	1.8785	14.68	4.37
	3	32.24°	2.4434	(101)	0.9537	16.12	8.72
	4	44.71°	1.8934	(102)	2.4575	22.35	3.5
	5	53.18°	1.6204	(110)	1.3697	26.59	6.48
	6	59.76°	1.4762	(103)	1.9896	29.88	4.60
	7	64.39°	1.3725	(112)	2.3911	32.19	3.92
Fruit	1	26.38°	3.0180	(100)	3.8908	13.19	2.09
	2	29.27°	2.5990	(002)	1.7332	14.63	4.74
	3	32.99°	2.4730	(101)	1.9235	16.42	4.31
	4	44.32°	1.9253	(102)	2.5506	22.16	3.36
	5	52.36°	1.6194	(110)	1.8683	26.18	4.74
	6	59.21°	1.4746	(103)	1.9214	29.60	4.76
	7	64.02°	1.4441	(112)	2.8621	32.01	3.27

be -15.0 mV and -18.9 mV indicated the moderate stability of ZnO NPs. The DLS stabiles of the biosynthesized ZnO NPs were found 244.6 d. nm leaves and 256.5 d. nm fruits extracts respectively.

Antibacterial activity of synthesized ZnO NPs in Well diffusion method

The antimicrobial activity of biosynthesized ZnO NPs using *B. tinctoria* leaves and fruits extract was studied at different concentrations (50,100 and 150 µg/mL) towards various human pathogenic bacteria gram-positive (*S. aureus, E. faecium*and and *E. faecalis*) and gram-negative (*E. coli, S. typhi* and *P. aeruginosa*) on agar well diffusion method and are represented in **Fig-3** and **4,** the zone of inhibition showed in **Table- 3.** The maximum zone of inhibition was observed in the *E. faecalis* (19 ± 0.5 mm) 150 µg/mL concentration of leaf-based NPs. Fruit-based synthesized NPs also have good antibacterial activity against *S. aureus, E. faecium* and *E. faecalis* of (19 ± 0.1 mm) the 150 µg/mL concentration. The more resistant bacteria of *E. coli* have (12 ± 0.1 mm) inhibition with a higher concentration of ZnO NPs and the positive control tetracycline 10 µg/mL (20 ± 0.1 mm to 25 ± 0.1 mm) also observed respectively. The negative control of distilled water does not observe any zone of inhibition. The zone of inhibition exhibited the disruption of the membrane with a high generation rate of surface oxygen species by the mechanism of the biocidal actions of ZnO NPs, finally lead to cell damage. Interestingly the size of the zone of inhibition was differed according to the method of biosynthesis, type of pathogens, and especially the concentration of ZnO NPs [36]. There was an increased inhibition growth while increasing ZnO NPs concentration because of its proper diffusion of drugs in the agar medium. While comparing with their stains, gram-positive bacteria were more effective than gram-negative bacteria. Besides the broad spectrum of antibacterial properties, nanoparticles have been used as a vector for the delivery of antimicrobial moieties that greatly influx the biocidal properties [37]. The plant extracts have active compounds like phenolics, flavonoids, saponins, and alkaloids with more antioxidants that can neutralize ROS, free radicals, and chelate metals. Hence, the antioxidants in plants are responsible for the metal or metal oxides green synthesis of NPs, by its reducing and stabilizing capacity. Accordingly, ZnO NPs have found that highly toxic to bacteria and only exhibit minimal effects on human cells, which recommended prospectus uses of agricultural and food industries.

Anti-biofilm activity

The Biofilm formation ability of *S. aureus*, *E. coli*, *S. typhi*, *P. aeruginosa*, *E. faecium,* and *E. faecalis* was described in previous reports [39-43]. Anti-biofilm inhibition activity of *B. tinctoria* leaves and fruits biosynthesized ZnO NPs, under *in vitro* conditions were observed with a MIC value of 40 µg/mL which has strong antibacterial activity. The present study tested with various concentration of sub- MIC doses (0, 10, 20, 30 µg/mL) of ZnO NPs incubated at 35 °C ± 2 °C for 48 hours. After incubation, planktonic cells were discarded from

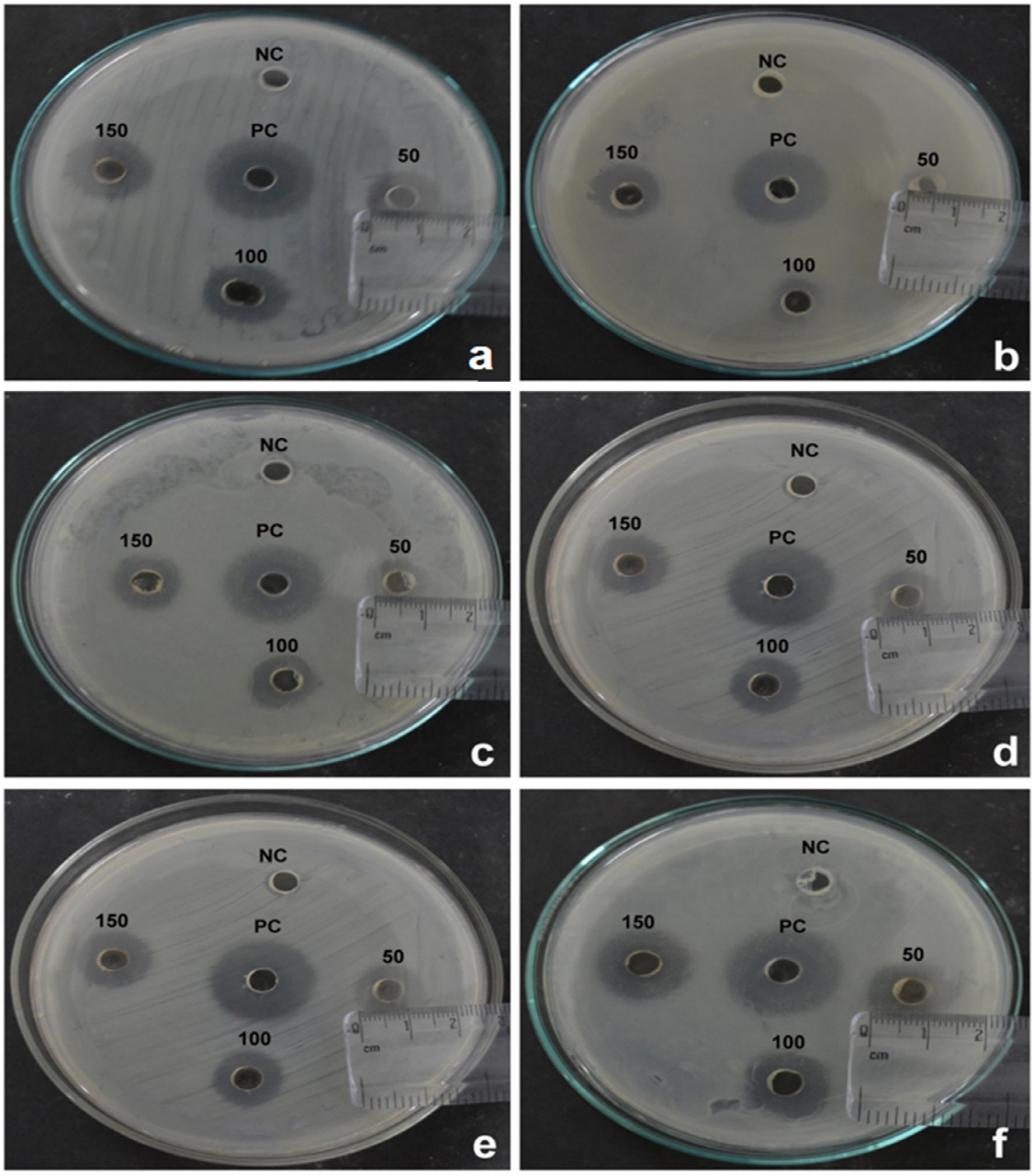

Fig. 3. Antibacterial activity of leaf based synthesis of ZnO NPs against **a**- S. aureus, **b**- *E. coli*, **c**- *S. typhi*, **d**- *P. aeruginosa*, **e**- *E. faecium* and **f**- *E. faecalis* in different concentration (50, 100, 150 µg/ml), **NC**- negative control and **PC**- positive control (tetracycline).

each growth, including the control (without treated ZnO NPs). The biofilm microbial formation on the glass surface was then stained with CV and biofilm formation significantly reduced in all the test tubes with increased ZnO NPs concentration (**Fig- 5**). Biofilms are complicated microorganism communities that show resistance to antibiotic action and are natural human immune resistance [44]. These infections are difficult to eradicate due to multidrug-resistant pathogens [45]. The control measures have some efficient strategies for their reduced growth rate and secretion of virulence factors that are required for preventing the development of harmful biofilms. The antibacterial activity depends on several factors mainly their vast surface area in contact with bacteria through Van

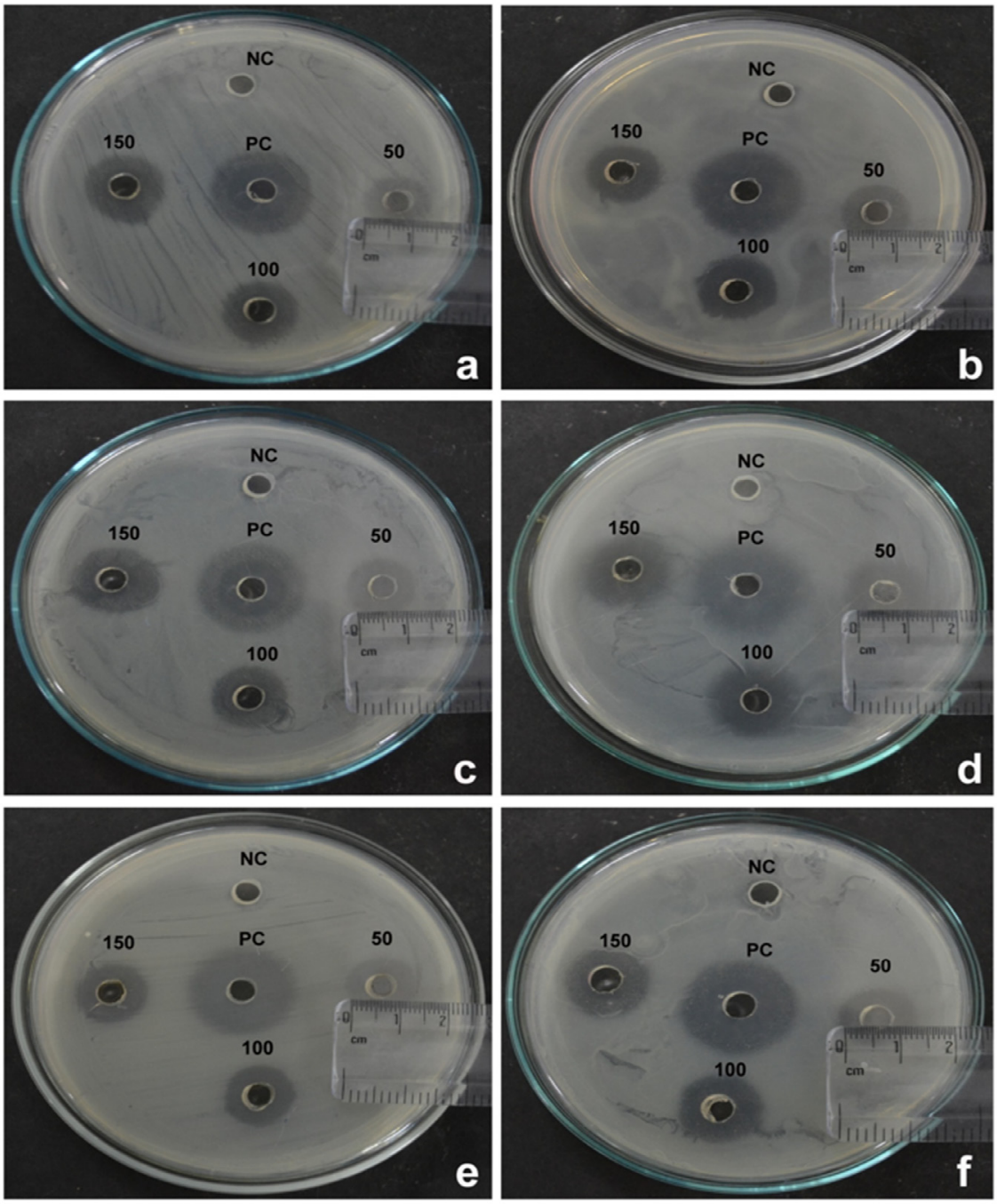

Fig. 4. Antibacterial activity of fruit based synthesis of ZnO NPs against **a**- S. aureus, **b**- *E. coli*, **c**- *S. typhi*, **d**- *P. aeruginosa*, **e**- *E. faecium* and **f**- *E. faecalis* in different concentration (50, 100, 150 µg/ml), **NC**- negative control and **PC**- positive control (tetracycline).

Der Waals forces or hydrophobic interactions and electrostatic attraction; also NPs size, stability, and together with the drug concentration against MDR bacteria [46]. The extent of microbial biofilm formation in the presence and absence of ZnO NPs was also measured by determining the amount of total extractable protein [47]. These results pointed out that ZnO NPs exhibited adequate to significant anti-biofilm activity against the six pathogenic bacteria at different concentrations (0, 10, 20, 30 µg/mL). The biofilm growth spectrum has been recorded in **Fig- 6** and bacterial biofilm always de-

Table 3. Antibacterial activities on ZnO NPs on leaf and fruit extracts

Berberis tinctoria Extracts		Microorganism	Gram Reaction	Zone of Inhibition (mm)				
				50 µg/mL	100 µg/mL	150 µg/mL	Positive control	Negative Control
Leaf	1	*S. aureus*	GPB	12±0.2	15±0.2	18±0.1	21±0.1	NA
	2	*E. coli*	GNB	8±0.5	10±0.2	12±0.1	20±0	NA
	3	*S. typhi*	GNB	15±0.5	16±0.1	18±0.2	20±0	NA
	4	*P. aeruginosa*	GNB	11±0.2	13±0.1	14±0.2	20±0.2	NA
	5	*E. faecium*	GPB	14±0.1	15±0.5	18±0.1	20±0.1	NA
	6	*E. faecalis*	GPB	15±0.3	16±0.4	19±0.5	20±0.1	NA
Fruit	1	*S. aureus*	GPB	14±0.1	17±0.2	19±0.1	21±0.1	NA
	2	*E. coli*	GNB	12±0.5	15±0.2	18±0	25±0.1	NA
	3	*S. typhi*	GNB	13±0.3	16±0.1	18±0.1	23±0.1	NA
	4	*P. aeruginosa*	GNB	12±0.1	14±0.1	16±0.1	20±0	NA
	5	*E. faecium*	GPB	13±0.1	17±0.1	19±0.1	20±0	NA
	6	*E. faecalis*	GPB	15±0.2	17±0.1	19±0.1	20±0	NA

The *in vitro* antibacterial assays were done in triplicates and the results were expressed as Mean ± Standard deviation (SD). Gram-Positive Bacteria (GPB) and Green Negative Bacteria (GNB).

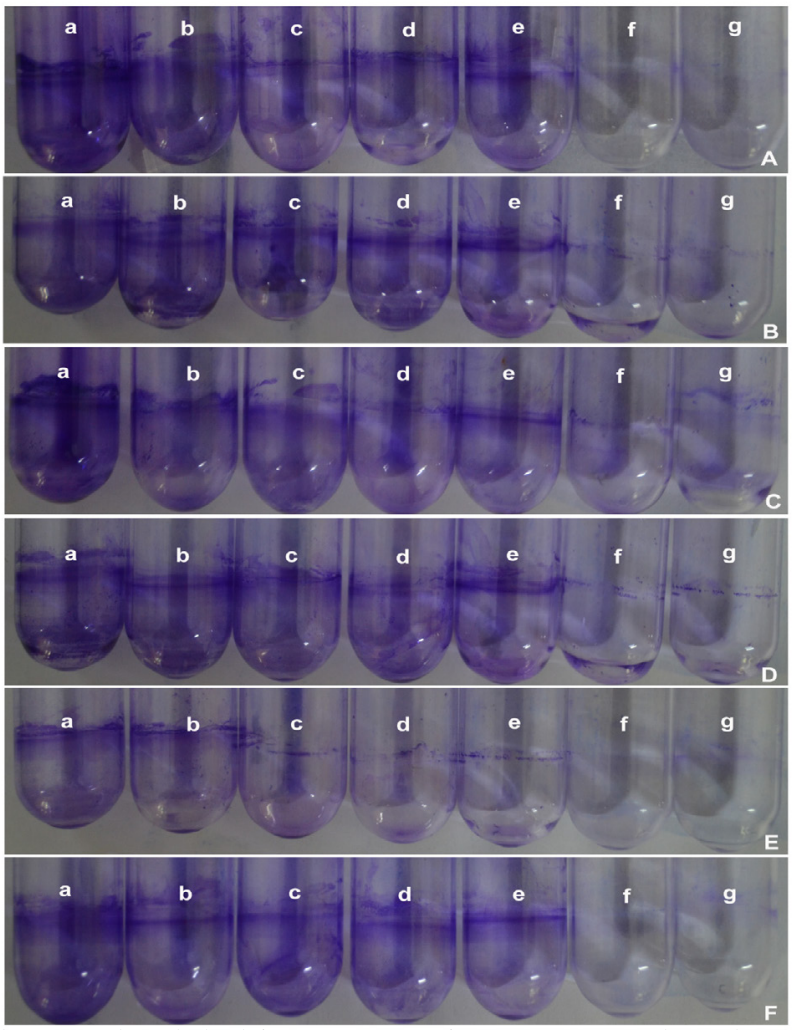

Fig. 5. Anti-biofilm detection in tube method in different concentration of ZnO NPs against six pathogenic bacteria **A**- *S. aureus*, **B**- *E. coli,* **C**- *S. typhi*, **D**- *P. aeruginosa*, **E**- *E. faecium* and **F**- *E. faecalis* (**a**- control, **b**- leaf 10 µg/ml, **c**- fruit 10 µg/ml, **d**- leaf 20 µg/ml, **e**- fruit 20 µg/ml, **f**- leaf 30 µg/ml and **g**- fruit 30 µg/ml).

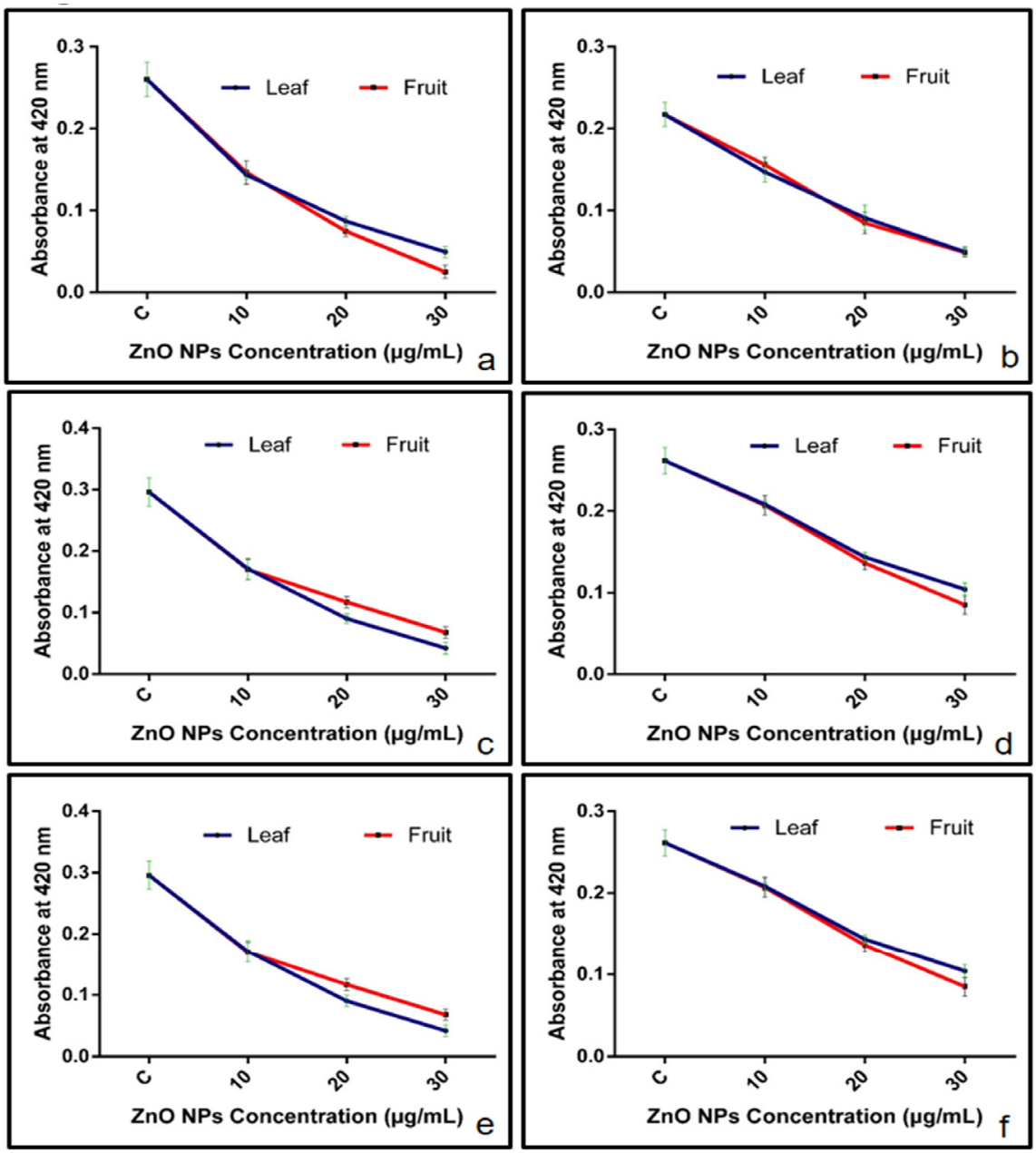

Fig. 6. Crystal violet staining of biofilm formation against the six pathogenic bacterial **a**- *S. aureus*, **b**- *E. coli*, **c**- *S. typhi*, **d**- *P. aeruginosa*, **e**- *E. faecium* and **f**- *E. faecalis* using leaf and fruit based synthesis of ZnO NPs. Biofilms were formed in the different concentration (0, 10, 20, 30 µg/ml) of ZnO NPs and quantified by CV staining. Error bar indicate standard deviation (±SD) of replicates.

pending on the ZnO NPs concentration. Presently the biofilms are untreated, antibiotics are ineffective, and many agents are failing to reach the target cells embedded deep inside the biofilm matrix. Therefore, an alternative path is needed to control the diseases involving biofilms [48]. Hence, *B. tinctoria* leaves and fruits-based biosynthesized ZnO NPs have proven to be against the biofilm formation hence it can recommend for the medical and food industries.

ZnO NPs inhibit microbial attachment

In this study, 100 µl of bacterial culture was inoculated in the sterile medium containing sterile coverslips. The different concentrations of ZnO NPs (0, 10, 20, 30 µg/mL) were added to the medium and incubated at 35 ± 2°C at 48 hours. After incubation coverslips were removed from the culture

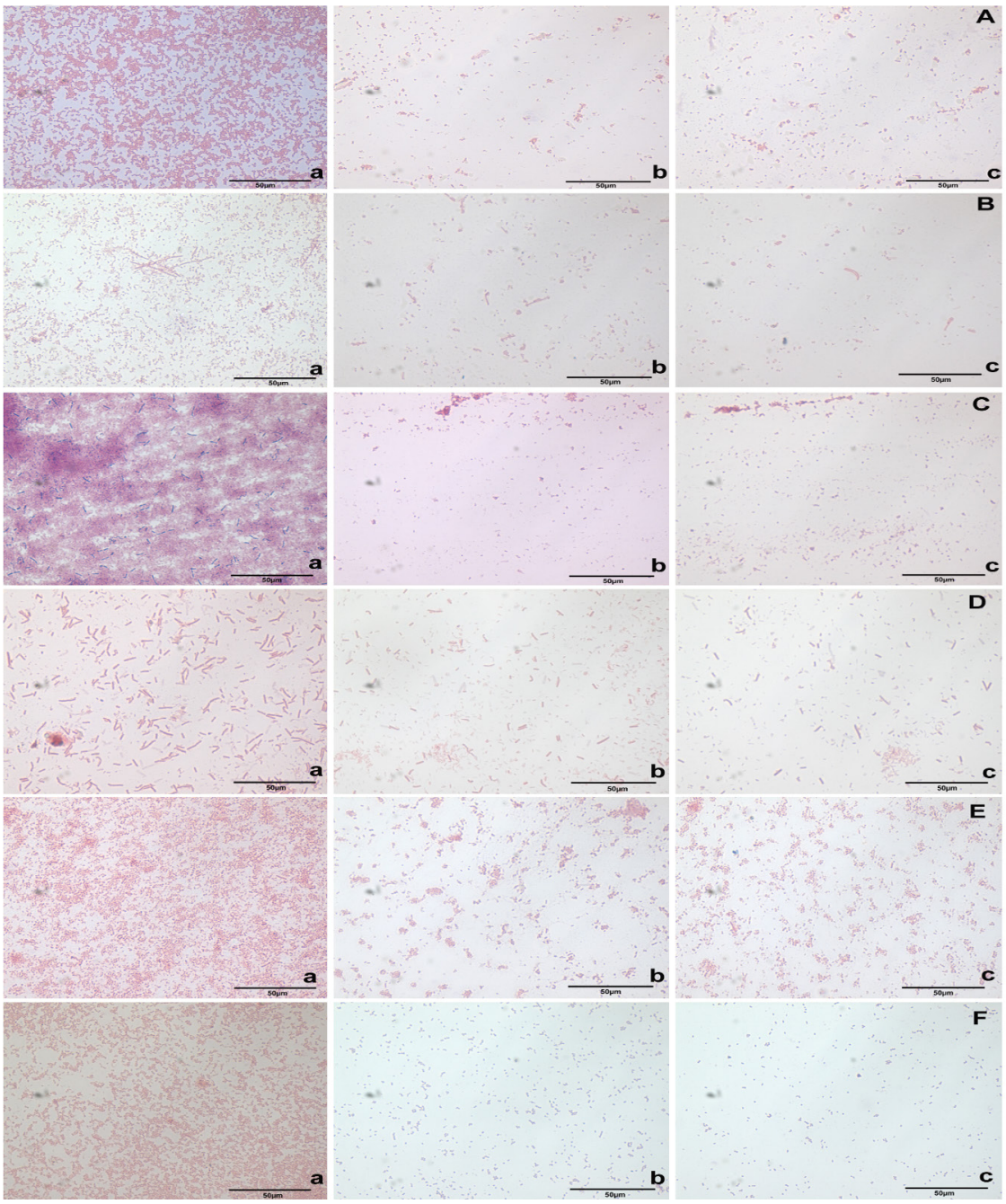

Fig. 7. Micrographs of Anti-biofilm detection to cover slips recovered from culture medium supplemented with different concentration of ZnO NPs against six pathogenic bacteria was examined by light microscopy. **A**- *S. aureus,* **B**- *E. coli,* **C**- *S. typhi*, **D**- P. aeruginosa, **E**- *E. faecium* and **F**- *E. faecalis* (**a**- control, **b**- leaf 30 µg/ml, **c**- fruit 30 µg/ml). Figures are representative of images obtained from thre e independent experiments and the microscopy image 40X magnification.

medium, stained with CV and acridine orange to observe the biofilms under the light microscope. In the control set of all pathogens bacterial showed a concentrated microbial biofilm growth on the glass surface (showed only on control set (0 µg/mL) and ZnO NPs 30 µg/mL of **Fig- 7**). The bacterial biofilm formation is endowed in several stages including the attachment of microcolony formation, maturation**,** and dispersion. The biofilm attenuation is the initial step of biofilm development by prevention of

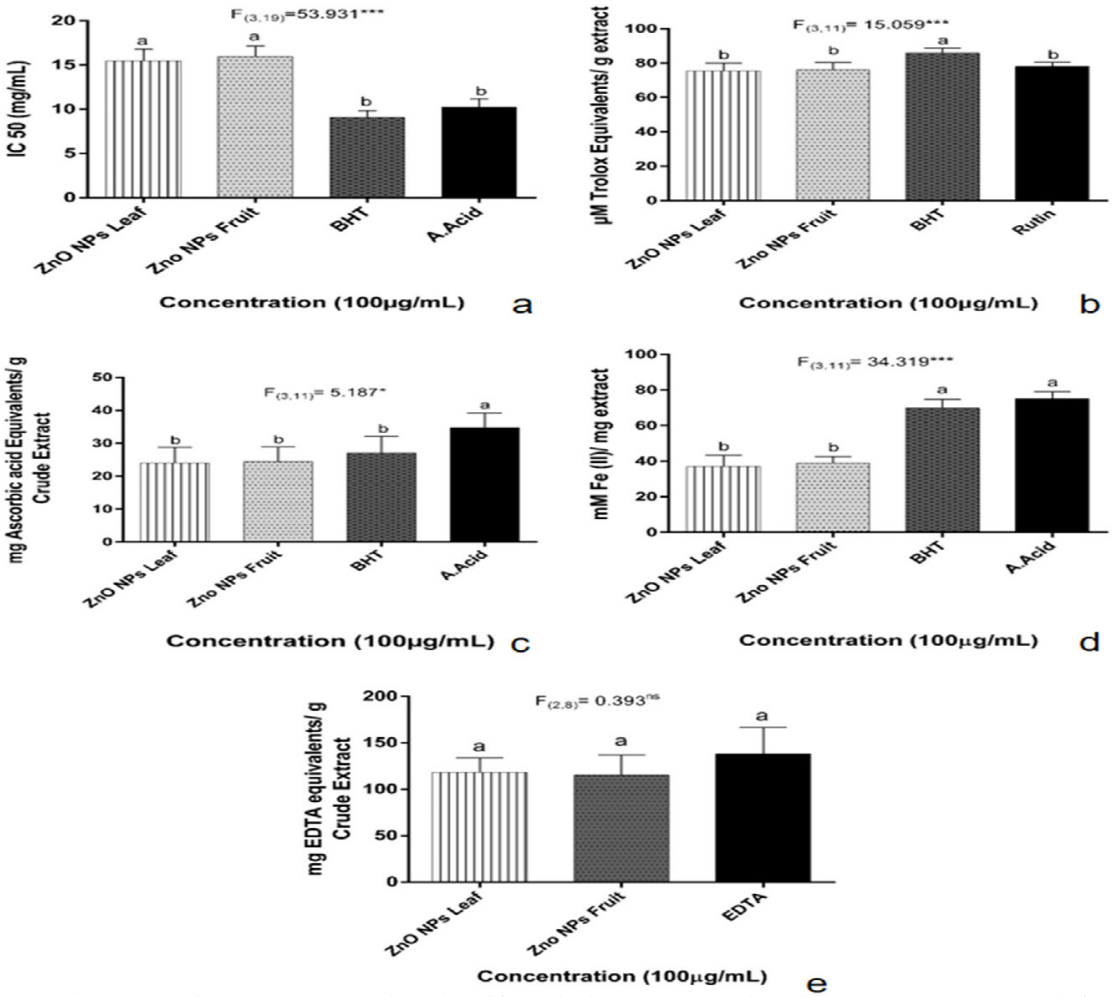

Fig. 8. **a.**The DPPH* radical assay was to test the ability of free radical scavengers to evaluate the IC_{50} values on *B. tinctoria* leaf and fruit based synthesis of ZnO NPs was compared with BHT and Ascorbic acid. **b**- The $ABTS^{\cdot}$+ scavenging activities on *B. tinctoria* leaf and fruit based synthesis of ZnO NPs was compared with BHT and rutin standard. **c**- The total antioxidants activity on phosphomolybdenum method on *B. tinctoria* leaf and fruit based synthesis of ZnO NPs was compared with BHT and Ascorbic acid. **d**- The FRAP activity on *B. tinctoria* leaf and fruit based synthesis of ZnO NPs in terms of Trolex equivalence to compared with BHT and rutin standard. **e**- The metal chelating activity of *B. tinctoria* leaf and fruit based synthesis of ZnO NPs was compared with EDTA equivalence. **BHT**- Butylated hydroxyl toluene: **A. acid**- Ascorbic acid; **EDTA**- Ethylene diamine tetra acetic acid. Data are presented as Mean ± SE followed by same letter (s) are not significantly (p >0.05) different according to DMRT. *** Significant at 0.1% level, *Significant at 5% level, ns- not significant.

bacterial attachment to the surfaces by ZnO NPs [49].

Antioxidant activities

DPPH radical scavenging activities of leaves and fruits synthesized ZnO NPs are shown in **Fig- 8 a**. The leaves (15.47 µg/mL) and fruits (15.96 µg/mL) based ZnO NPs showed better IC_{50} values for $DPPH^{\cdot}$ radical scavenging activities. The IC_{50} of standard synthetic antioxidant BHT was found to be (9.12 µg/mL) minimal. Whereas, natural antioxidant as ascorbic acid (10.25 µg/mL) was found to be much better than that of ZnO NPs. The result indicated the potential free radical scavenging activity in a dose-dependent manner. In *B. aristata* also similar results have been reported [32]. The radical scavenging activities of the synthesized ZnO NPs were showed an IC_{50} value of (127.74 µg/mL) [50].

The results of $ABTS^{\cdot+}$cation radical scavenging activities of leaves and fruits synthesized ZnO NPs are shown in **Fig- 8 b**. The ABTS cation radical scavenging activities of leaves based ZnO NPs

(75.47 µM Trolox equivalents/g extract respectively) and fruits -based ZnO NPs 76.03 µM Trolox equivalents/g extract respectively) compared with standards BHT (85.87 µM Trolox equivalents/ g extract) and rutin (78.03 µM Trolox equivalents/g extract respectively). The ABTS radicals exhibiting their highest activity (93.25%) at a concentration (100 µM) were reported as the ZnO NPs of Caffeic acid-functionalized ZnO NPs [51]. The results indicated that ZnO NPs have a strong ability to do-

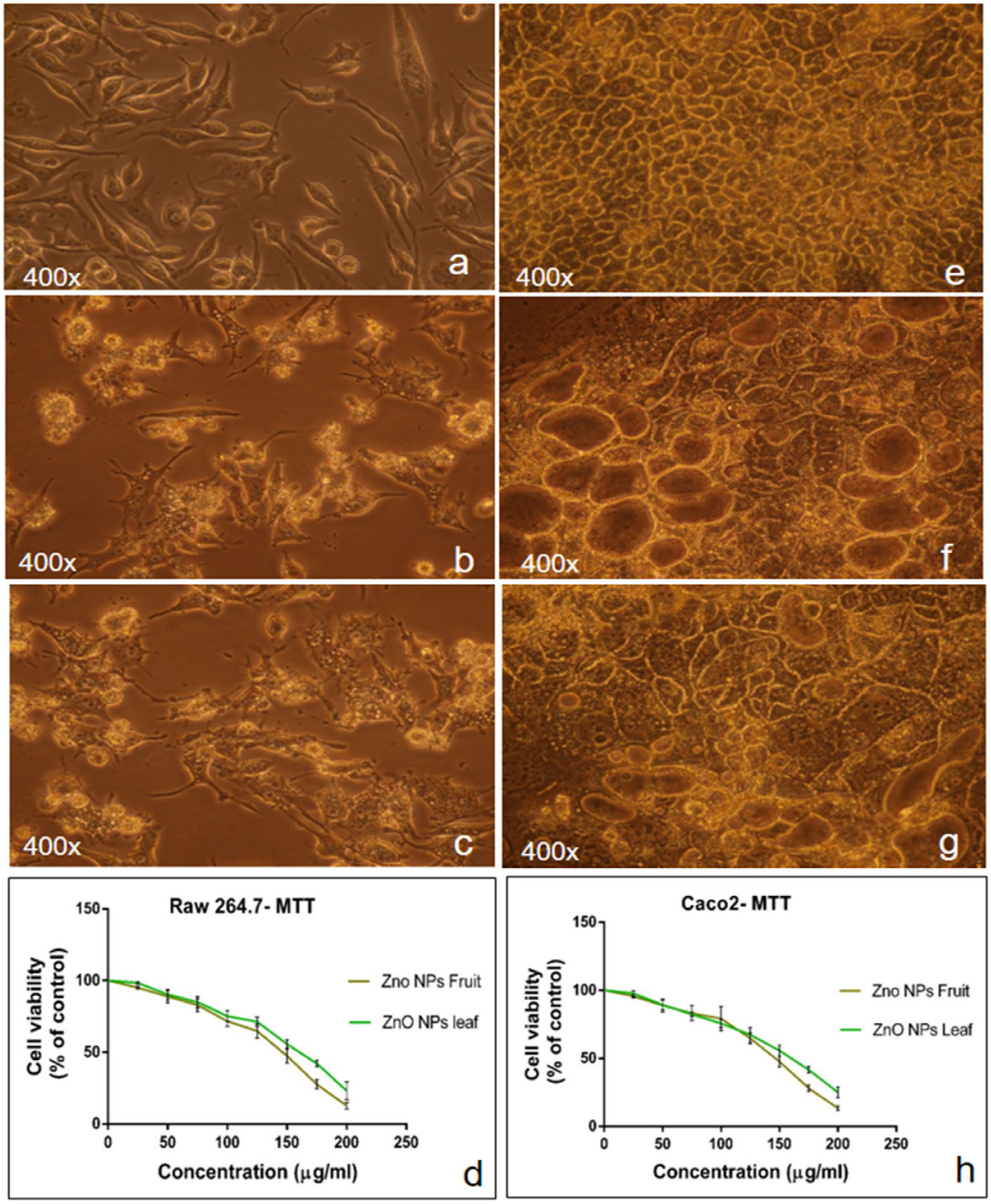

Fig. 9. Morphology of the Raw 264.7 and Caco-2 cancer cells- treated samples, **a** and **e**- control, **b** and **f**- leaf synthesized ZnO NPs, and **c** and **g**- fruit synthesized ZnO NPs. **d** and **h** - IC_{50} values of cell viability on leaf and fruit synthesized ZnO NPs of various concentrations. Error bar indicate standard deviation (± SD) of replicates. **IC_{50}**- half-maximal inhibitory concentration.

nate hydrogen and could serve as primary antioxidants to scavenge free radicals.

The total antioxidant activity was analyzed by the phophomolybdenum method using both extracts of leaves (24.03 mg AAE/ g extract) and fruits (24.36 mg AAE/ g extract) ZnO NPs and shown in **Fig- 8 c**. Total antioxidant capacity observed for the ZnO NPs can be correlated with its free radical scavenging activity equivalent to that of ascorbic acid (34.72 mg AAE/ g extract) and BHT (27.10 mg AAE/ g extract). The phosphomolybdenum assays of the total antioxidant capacity of ZnO NPs were found to be 70% by using an algal-based synthesis of nanoparticles [52].

The antioxidant potential of leaves and fruits synthesized ZnO NPs were estimated from their ability to reduce TPTZ- Fe (III) complex to TPTZ-Fe (II) and are shown in **Fig- 8 d.** It measures the antioxidant effect of any substance in the reaction medium as reducing ability. The leaves biosynthesized nanoparticles (37.03 mM Fe (II)/ mg extract) and fruits (39.02 mM Fe (II)/ mg extract) showed the highest ferric reducing power. The standard antioxidants BHT and A. Acid were found to that efficient antioxidant potential rather than ZnO NPs. Algal-based synthesized nanoparticles have 73% total antioxidant capacity [52].

Iron is a fundamental metal for normal physiology to undergo Fenton reaction, these reduced metals may form highly harmful hydroxyl radicals and thereby contributing to oxidative stress [53]. Metal chelating activity was significant as it reduced the concentration of the metal catalyzing transition in oxidative degradation of lipids. According to **Fig- 8 e**, metal chelating activity was showed in leaves (115.17 mg EDTA equivalents/ g extract) and fruits (118.21 mg EDTA equivalents/ g extract), due to the capping of biomolecules. Hence, antioxidant**s** may be related to its sequestering of Fe^{2+} ions catalyze Fenton-type reactions or participate in metal-catalyzed hydrogen peroxide decomposition reactions. Already reported that ZnO NPs concentrations were proportional to the antioxidants that overcome the action by free radicals. Therefore, it allows the system to deal expressively with viruses thereby improving the body's immune systems [54]. Nowadays, it will be useful for increase the immune power of the human body to preventing infectious diseases.

In vitro cytotoxicity by MTT assay

MTT assay was analyzed to determine the biocompatibility and potential effect of the green synthesized ZnO NPs for biomedical uses. The various NPs also have the potential effects of cytotoxic towards the various cancer cell lines. As well as the cytotoxicity effects of NPs mainly depend on the concentration, shape, size, and surface modifications. The cytotoxic activity of ZnO NPs has evaluated by MTT assay on the two different cell lines Raw 264.7 and Caco-2. The assay was performed to determine the ZnO NP's toxic effect on the treated cancer cells with various concentrations in Raw 264.7 and Caco-2 Cells showed in **Fig-9**. The best activity was observed in fruits synthesized ZnO NPs with IC_{50} (Raw 264.7- 136.55 µg/mL and Caco-2- 154.21 µg/mL). The leaves synthesized ZnO NPs IC_{50} value is (Raw 264.7- 142.18 µg/mL and Caco-2- 158.17 µg/mL). The MTT assay was achieved to determine the biocompatibility and potential effect of the green synthesized ZnO NPs for biomedical uses. The ZnO NPs of cytotoxicity effect on Rajan et al., already reported the Caco-2 human colon cell lines always depend on the size and surface modifications [55]. It confirms that green synthesized ZnO NPs exhibited a good anti-proliferation effect and excellent biocompatibility in both cell lines, signifying their impotent role in biomedical applications.

CONCLUSION

This present study deals with the green synthesis of ZnO NPs using leaf and fruit extracts of *Berberis tinctoria.* The synthesized nanomaterial was characterized by UV-visible spectroscopy, FTIR, XRD, SEM, EDX, DLS, and ZETA potential determination analysis revealed the optical properties and structural properties of ZnO NPs. The promising antibacterial agent due to ZnO NPs activity against both gram-positive and gram-negative bacteria. The introduction of biofilm attenuating agents may allow therapeutic approaches against biofilm-associated human infections. As well as the anti-cancer effects also defending the concentration, size, shape, and surface morphology. Morphologically distinct of the biological activity of fruit ZnO NPs showed significant results with concentration-dependent. The ZnO NPs may work as part of combination therapy against the human pathogenic bacteria and multi-drug resistance bacteria. Moreover, the antioxidant property of ZnO NPs could allow them to use in textiles, health care products, and more importantly preparation of nanomedicine. ZnO NPs are safe up to a certain

level but may become toxic at higher concentrations. Compared with other metal oxide nanoparticles, ZnO NPs are inexpensive and relatively less toxic with excellent biomedical applications, such as drug delivery, diabetes treatment; anti-inflammation; wound healing, anticancer and antimicrobial agents in food preservation industries.

ACKNOWLEDGMENTS

The present study was supported by Tamil Nadu State Council Science and Technology, Chennai, Tamil Nadu. India (TNSCST/&T Project/AS/RJ/2013-2014) and Dr. T. Muthukumar, Associate Professor, Department of Botany, Bharathiar University, Coimbatore for providing microscopy facilities.

CONFLICT OF INTEREST

The authors declare no conflict of interest.

REFERENCE

1. Kanniah P, Radhamani J, Chelliah P, Muthusamy N, Joshua Jebasingh Sathiya Balasingh E, Reeta Thangapandi J, et al. Green Synthesis of Multifaceted Silver Nanoparticles Using the Flower Extract of Aerva lanata and Evaluation of Its Biological and Environmental Applications. ChemistrySelect. 2020;5(7):2322-31.
2. Khan ZUH, Khan A, Chen YM, Shah NS, Khan AU, Muhammad N, et al. Enhanced antimicrobial, anti-oxidant applications of green synthesized AgNPs- an acute chronic toxicity study of phenolic azo dyes & study of materials surface using X-ray photoelectron spectroscopy. Journal of Photochemistry and Photobiology B: Biology. 2018;180:208-17.
3. Jones MR, Osberg KD, Macfarlane RJ, Langille MR, Mirkin CA. Templated Techniques for the Synthesis and Assembly of Plasmonic Nanostructures. Chemical Reviews. 2011;111(6):3736-827.
4. Roduner E. Size matters: why nanomaterials are different. Chemical Society Reviews. 2006;35(7):583.
5. Sharma D, Ledwani L, Mehrotra T, Kumar N, Pervaiz N, Kumar R. Biosynthesis of hematite nanoparticles using Rheum emodi and their antimicrobial and anticancerous effects in vitro. Journal of Photochemistry and Photobiology B: Biology. 2020;206:111841.
6. Sundrarajan M, Ambika S, Bharathi K. Plant-extract mediated synthesis of ZnO nanoparticles using Pongamia pinnata and their activity against pathogenic bacteria. Advanced Powder Technology. 2015;26(5):1294-9.
7. Wang Z, Que B, Gan J, Guo H, Chen Q, Zheng L, et al. Zinc oxide nanoparticles synthesized from Fraxinus rhynchophylla extract by green route method attenuates the chemical and heat induced neurogenic and inflammatory pain models in mice. Journal of Photochemistry and Photobiology B: Biology. 2020;202:111668.
8. Ahmed S, Ahmad M, Swami BL, Ikram S. A review on plants extract mediated synthesis of silver nanoparticles for antimicrobial applications: A green expertise. Journal of Advanced Research. 2016;7(1):17-28.
9. Peterson E, Kaur P. Antibiotic Resistance Mechanisms in Bacteria: Relationships Between Resistance Determinants of Antibiotic Producers, Environmental Bacteria, and Clinical Pathogens. Frontiers in Microbiology. 2018;9.
10. Ali SG, Ansari MA, Alzohairy MA, Alomary MN, Jalal M, AlYahya S, et al. Effect of Biosynthesized ZnO Nanoparticles on Multi-Drug Resistant Pseudomonas Aeruginosa. Antibiotics. 2020;9(5):260.
11. Johnson LR. Microcolony and biofilm formation as a survival strategy for bacteria. Journal of Theoretical Biology. 2008;251(1):24-34.
12. Ołdak E, Trafny EbA. Secretion of Proteases by Pseudomonas aeruginosa Biofilms Exposed to Ciprofloxacin. Antimicrobial Agents and Chemotherapy. 2005;49(8):3281-8.
13. Joo H-S, Otto M. Molecular Basis of In Vivo Biofilm Formation by Bacterial Pathogens. Chemistry & Biology. 2012;19(12):1503-13.
14. Vasudevan R. Biofilms: Microbial Cities of Scientific Significance. Journal of Microbiology & Experimentation. 2014;1(3).
15. Pati R, Mehta RK, Mohanty S, Padhi A, Sengupta M, Vaseeharan B, et al. Topical application of zinc oxide nanoparticles reduces bacterial skin infection in mice and exhibits antibacterial activity by inducing oxidative stress response and cell membrane disintegration in macrophages. Nanomedicine: Nanotechnology, Biology and Medicine. 2014;10(6):1195-208.
16. Balan K, Qing W, Wang Y, Liu X, Palvannan T, Wang Y, et al. Antidiabetic activity of silver nanoparticles from green synthesis using Lonicera japonica leaf extract. RSC Advances. 2016;6(46):40162-8.
17. Park TS, Donnenberg VS, Donnenberg AD, Zambidis ET, Zimmerlin L. Dynamic Interactions Between Cancer Stem Cells and Their Stromal Partners. Current Pathobiology Reports. 2014;2(1):41-52.
18. Selim YA, Azb MA, Ragab I, H. M. Abd El-Azim M. Green Synthesis of Zinc Oxide Nanoparticles Using Aqueous Extract of Deverra tortuosa and their Cytotoxic Activities. Scientific Reports. 2020;10(1).
19. Cheng J, Wang X, Qiu L, Li Y, Marraiki N, Elgorban AM, et al. Green synthesized zinc oxide nanoparticles regulates the apoptotic expression in bone cancer cells MG-63 cells. Journal of Photochemistry and Photobiology B: Biology. 2020;202:111644.
20. Fyson PF. The Flora of the Nilgiris and Pulney HillTops, Bishen Singhnand Mahendra Pal Singh, Dehradun,. 1974;Vol. 1.:37- 39.
21. Srivastava S, Srivastava M, Misra A, Pandey G, Rawat A. A review on biological and chemical diversity in *Berberis* (Berberidaceae). EXCLI journal, 2015;14:247.
22. Santhoshkumar J, Kumar SV, Rajeshkumar S. Synthesis of zinc oxide nanoparticles using plant leaf extract against urinary tract infection pathogen. Resource-Efficient Technologies. 2017;3(4):459-65.
23. Azam A, Ahmed, Oves, Khan, Habib, Memic A. Antimicrobial activity of metal oxide nanoparticles against Gram-positive and Gram-negative bacteria: a comparative study. International Journal of Nanomedicine. 2012:6003.
24. Bhattacharyya P, Agarwal B, Goswami M, Maiti D, Baruah S, Tribedi P. Zinc oxide nanoparticle inhibits the biofilm formation of Streptococcus pneumoniae. Antonie van Leeuwenhoek. 2017;111(1):89-99.

25. Braca A, De Tommasi N, Di Bari L, Pizza C, Politi M, Morelli I. Antioxidant Principles fromBauhiniatarapotensis. Journal of Natural Products. 2001;64(7):892-5.
26. Re R, Pellegrini N, Proteggente A, Pannala A, Yang M, Rice-Evans C. Antioxidant activity applying an improved ABTS radical cation decolorization assay. Free Radical Biology and Medicine. 1999;26(9-10):1231-7.
27. Prieto P, Pineda M, Aguilar M. Spectrophotometric Quantitation of Antioxidant Capacity through the Formation of a Phosphomolybdenum Complex: Specific Application to the Determination of Vitamin E. Analytical Biochemistry. 1999;269(2):337-41.
28. Pulido R, Bravo L, Saura-Calixto F. Antioxidant Activity of Dietary Polyphenols As Determined by a Modified Ferric Reducing/Antioxidant Power Assay. Journal of Agricultural and Food Chemistry. 2000;48(8):3396-402.
29. Dinis TCP, Madeira VMC, Almeida LM. Action of Phenolic Derivatives (Acetaminophen, Salicylate, and 5-Aminosalicylate) as Inhibitors of Membrane Lipid Peroxidation and as Peroxyl Radical Scavengers. Archives of Biochemistry and Biophysics. 1994;315(1):161-9.
30. Mosmann T. Rapid colorimetric assay for cellular growth and survival: Application to proliferation and cytotoxicity assays. Journal of Immunological Methods. 1983;65(1-2):55-63.
31. Al-Dhabi N, Valan Arasu M. Environmentally-Friendly Green Approach for the Production of Zinc Oxide Nanoparticles and Their Anti-Fungal, Ovicidal, and Larvicidal Properties. Nanomaterials. 2018;8(7):500.
32. Chandra H, Patel D, Kumari P, Jangwan JS, Yadav S. Phyto-mediated synthesis of zinc oxide nanoparticles of Berberis aristata: Characterization, antioxidant activity and antibacterial activity with special reference to urinary tract pathogens. Materials Science and Engineering: C. 2019;102:212-20.
33. Senthilkumar N, NandhaKumar E, Priya P, Soni D, Vimalan M, Potheher IV. Synthesis, anti-bacterial, anti-arthritic, anti-oxidant and *In-vitro* cytotoxicity activities of ZnO nanoparticles using leaf extract of *Tectona grandis* (L.). New Journal of Chemistry, 2017;41:10347-10356.
34. Selvarajan E, Mohanasrinivasan V. Biosynthesis and characterization of ZnO nanoparticles using Lactobacillus plantarum VITES07. Materials Letters. 2013;112:180-2.
35. Kokila K, Elavarasan N, Sujatha V. Diospyros montana leaf extract-mediated synthesis of selenium nanoparticles and their biological applications. New Journal of Chemistry. 2017;41(15):7481-90.
36. Wahab R, Kim Y-S, Mishra A, Yun S-I, Shin H-S. Formation of ZnO Micro-Flowers Prepared via Solution Process and their Antibacterial Activity. Nanoscale Research Letters. 2010;5(10):1675-81.
37. Hadiya S, Liu X, Abd El-Hammed W, Elsabahy M, Aly SA. Levofloxacin-Loaded Nanoparticles Decrease Emergence of Fluoroquinolone Resistance in Escherichia coli. Microbial Drug Resistance. 2018;24(8):1098-107.
38. Bandeira M, Giovanela M, Roesch-Ely M, Devine DM, da Silva Crespo J. Green synthesis of zinc oxide nanoparticles: A review of the synthesis methodology and mechanism of formation. Sustainable Chemistry and Pharmacy. 2020;15:100223.
39. Miao J, Lin S, Soteyome T, Peters BM, Li Y, Chen H, et al. Biofilm Formation of Staphylococcus aureus under Food Heat Processing Conditions: First Report on CML Production within Biofilm. Scientific Reports. 2019;9(1).
40. Reisner A, Krogfelt KA, Klein BM, Zechner EL, Molin S. In Vitro Biofilm Formation of Commensal and Pathogenic Escherichia coli Strains: Impact of Environmental and Genetic Factors. Journal of Bacteriology. 2006;188(10):3572-81.
41. Di Domenico EG, Cavallo I, Pontone M, Toma L, Ensoli F. Biofilm Producing Salmonella Typhi: Chronic Colonization and Development of Gallbladder Cancer. International Journal of Molecular Sciences. 2017;18(9):1887.
42. Milivojevic D, Šumonja N, Medić S, Pavic A, Moric I, Vasiljevic B, et al. Biofilm-forming ability and infection potential of Pseudomonas aeruginosa strains isolated from animals and humans. Pathogens and Disease. 2018;76(4).
43. Rosa R, Creti R, Venditti M, D'Amelio R, Arciola CR, Montanaro L, et al. Relationship between biofilm formation, the enterococcal surface protein (Esp) and gelatinase in clinical isolates ofEnterococcus faecalisandEnterococcus faecium. FEMS Microbiology Letters. 2006;256(1):145-50.
44. Høiby N, Bjarnsholt T, Givskov M, Molin S, Ciofu O. Antibiotic resistance of bacterial biofilms. International Journal of Antimicrobial Agents. 2010;35(4):322-32.
45. Markowska K, Grudniak AM, Wolska KI. Silver nanoparticles as an alternative strategy against bacterial biofilms. Acta Biochimica Polonica, 2013;60 (4).
46. Li H, Chen Q, Zhao J, Urmila K. Enhancing the antimicrobial activity of natural extraction using the synthetic ultrasmall metal nanoparticles. Scientific Reports. 2015;5(1).
47. Tribedi P, Sil AK. Low-density polyethylene degradation by Pseudomonas sp. AKS2 biofilm. Environmental Science and Pollution Research. 2012;20(6):4146-53.
48. LewisOscar F, MubarakAli D, Nithya C, Priyanka R, Gopinath V, Alharbi NS, et al. One pot synthesis and anti-biofilm potential of copper nanoparticles (CuNPs) against clinical strains of Pseudomonas aeruginosa. Biofouling. 2015;31(4):379-91.
49. Lau PCY, Lindhout T, Beveridge TJ, Dutcher JR, Lam JS. Differential Lipopolysaccharide Core Capping Leads to Quantitative and Correlated Modifications of Mechanical and Structural Properties in Pseudomonas aeruginosa Biofilms. Journal of Bacteriology. 2009;191(21):6618-31.
50. Safawo T, Sandeep BV, Pola S, Tadesse A. Synthesis and characterization of zinc oxide nanoparticles using tuber extract of anchote (Coccinia abyssinica (Lam.) Cong.) for antimicrobial and antioxidant activity assessment. OpenNano. 2018;3:56-63.
51. Choi K-H, Nam K, Lee S-Y, Cho G, Jung J-S, Kim H-J, et al. Antioxidant Potential and Antibacterial Efficiency of Caffeic Acid-Functionalized ZnO Nanoparticles. Nanomaterials. 2017;7(6):148.
52. R KR, Durairaj B. EVALUATION OF THE ANTITYROSINASE AND ANTIOXIDANT POTENTIAL OF ZINC OXIDE NANOPARTICLES SYNTHESIZED FROM THE BROWN SEAWEED-TURBINARIA CONOIDES. International Journal of Applied Pharmaceutics. 2017;9(5):116.
53. Hippeli S, Elstner EF. Inhibition of Biochemical Model Reactions for Inflammatory Processes by Plant Extracts: A Review on Recent Developments. Free Radical Research. 1999;31(sup1):81-7.
54. Khan ZUH, Sadiq HM, Shah NS, Khan AU, Muhammad N, Hassan SU, et al. Greener synthesis of zinc oxide nanoparticles using Trianthema portulacastrum extract and evaluation of its photocatalytic and biological applications.

Journal of Photochemistry and Photobiology B: Biology. 2019;192:147-57.
55. Rajan M, Anthuvan AJ, Muniyandi K, Kalagatur NK, Shanmugam S, Sathyanarayanan S, et al. Comparative Study of Biological (Phoenix loureiroi Fruit) and Chemical Synthesis of Chitosan-Encapsulated Zinc Oxide Nanoparticles and their Biological Properties. Arabian Journal for Science and Engineering. 2019;45(1):15-28.